Research Article

Evaluating liquefaction induced settlement of shallow foundation on layered soil deposit

Ali Besharatinezhad[1] · Mohammad Ali Khodabandeh[1] · Raza Naderi[2]

Received: 28 August 2019 / Accepted: 22 October 2019 / Published online: 26 October 2019

Abstract
The occurrence of liquefaction in saturated layered soil deposit underlying the shallow foundation can cause a wide range of problems from settlement to tilting of structures and foundations. It this study in order to evaluate the liquefaction induced settlement of shallow foundation on the ground surface of layered soil deposit, numerical studies have accomplished. The soil deposit involves a continuous saturated fine sand that is sandwiched between two dense continuous sand layers and the whole system had been subjected to a base shaking. The settlement of shallow foundation has been evaluated by considering the influence of relative density (Dr) of middle sand layer. The variation of relative density of middle continuous soil layer was examined by using the finite element method in OpenSEES software. It was observed that the liquefaction has occurred up to the depth of 6 m. In addition, by examining the slope of the settlement–relative density curve, it was found that in continuous fine sand layer for relative densities higher than 60% the effect of this layer on settlement of shallow foundation can be neglected, but for relative densities less than 60% the slope of curve is sharper and as a result, the shallow foundation is experienced higher settlement with 17 cm for Dr = 40% in compare with settlement 10 cm for a uniform soil deposit with Dr = 75%.

Keywords Liquefaction · Settlement · Shallow foundation · Sand · OpenSEES

1 Introduction

One of the most hazardous effects of earthquake-induced phenomena is soil liquefaction. Soil liquefaction during an earthquake leads to the loss of hardness of the soil, which occurs mostly in saturated sands. A saturated sand layer when placed under dynamic loading tends to be denser and less voluminous. If it is not possible to drain the pore water under dynamic load, the pore water pressure gradually increases, if the water pressure is so high, the liquefaction phenomenon occurs when the pore pressure is equal to the total stress. In fact, in this case, the effective stress is zero and the sandy soil in this area does not have shear resistance and acts like a fluid [23].

Soil liquefaction during earthquake causes huge damage to a wide range of structures [16]. The phenomenon of liquefaction has consistently and historically impacted the buildings and structures, but seriously after the earthquake of Japan's Niigata in 1964 (with an intensity of 7.5 and in depth of 40 km), it was considered by scientific communities. It is notable that in earthquake of Japan's Niigata in 1964, the depth of the earthquake was high and the intensity of the earthquake was not much compared to the previous earthquakes. Therefore, due to the scale of the damage, there was probably another factors involved, which was the liquefaction phenomenon [9].

In the last few years, experimental and numerical studies in layered soil deposit with considering liquefaction phenomenon has been done. Several experimental studies

✉ Ali Besharatinezhad, Besharat71@gmail.com | [1]Geotechnical Engineering, Shahrood University of Technology, Shahrood, Iran. [2]Civil Engineering Department, Shahrood University of Technology, Shahrood, Iran.

based on physical model tests such as one-dimensional column test [10] and centrifuge tests [18] were conducted in order to evaluate the effects of liquefaction in layered sands. Fiegel and Kutter [7] studied the liquefaction mechanism for layered soils, in this study the layered soil model was consisted of fine sand layer that it was overlain by a layer of relatively impermeable silica flour (silt). The result of the model tests involving layered soils suggested that during liquefaction a water interlayer or very loose zone of soils may develop at the sand-silt interface due to the differences in permeability [7]. The results of dynamic centrifuge model tests were conducted by Maharjan and Takahashi [20] in order to investigate the liquefaction mechanism in non-homogeneous soil deposits. It was found that more excess pore water pressure (EPWP) remains for a longer period of time in the discontinuous region in non-homogeneous soil deposits compared with the continuous layered and uniform soil deposits. The rapid dissipation of EPWP through the discontinuous part in the non-homogeneous soil deposits manifests as a larger settlement in the discontinuous part, causing non-uniform settlements [20]. Liu and Qiao [13] performed several shaking table tests on layered soil in plane strain condition, and examined the effects of contact pressure and the peak ground acceleration. They concluded that the increment of the contact pressure in a constant peak ground acceleration causes a decrease in pore pressure ratio. Liu [14] did some centrifuge experiments to study the effects of permeability and relative density and it was concluded that higher settlements would occur in looser sands and the permeability had a major influence on the pore pressure generation. Dashti et al. [4] by conducting several centrifuge tests in layered soil, discussed two different mechanisms that participate in shallow foundation settlement. As far as numerical approach is concerned, there are a lot of papers that have tried to evaluate liquefaction induced settlement with numerical approach, but most of them were in homogenous soil deposit. For example, Koutsourelakis [11], Popescu et al. [21], and Lopez-Caballero and Modaressi Farahmand-Razavi [15] conducted 2D (plane strain) coupled finite element analysis to study the dynamic interaction between a homogenous liquefying soil layer and a structure resting on the ground surface. Karimi and Dashti [8] evaluated the predictive capabilities of a state-of-the-art numerical tool with the result of centrifuge experiments of a shallow foundation on a layered liquefiable soil deposit. There are two centrifuge tests in this study with different relative density for their liquefiable soil layer, but the effect of changing relative density for this layer on settlement of shallow foundation was not taken into account in particular.

Meherzad et al. [19] evaluated the performance of two shallow foundations with different contact pressures in liquefaction and in order to avoid complete collapse of the structure that has been built on liquefiable soil. Reece et al. [22] introduced a Geogrid at a certain depth below the foundation and this numerical study was modeled with a container consisting of uniform soil deposit. Ayoubi and Pak [1] studied the settlement of shallow footing on two-layered subsoil strata under earthquake loading with numerical approach. The Results showed that the presence of dense layer can mitigate the settlement up to 50% in comparison with uniform liquefiable layer [1]. Kumar and Kumari [12] numerically modeled the behavior of shallow foundation on liquefiable soil with using Biot basic theory of porous media. The results showed that settlement of foundations increased with the increase of soil permeability, excess pore pressure increases with the depth and decreases with the increases in shear modulus.

In this study, the settlement caused by liquefaction for shallow foundation on saturated layered soil deposit has been conducted with OpenSEES software. The pressure-dependent multi yield (PDMY) material has been used to assign soil properties. The model is consisted of layered saturated sandy soil and Biot theory [2] for saturated soils in a two-phase flow has been used. The model consists of three continuous layers of saturated soil in the thickness of 2, 3 and 25 m from top to bottom, respectively. The layers with thickness of 2 and 25 m have a constant relative density of 75% and by changing the relative density of the 3 m intermediate layer, the settlement, pore water pressure and excess pore water pressure (r_u) were measured. The time history of the settlement at different densities of the middle layer has been measured and compared with each other. Finally, the effect of the relative density of the intermediate-layer on the final settlement of the shallow foundation has been discussed.

2 Materials and methods

2.1 Methods and formulas used in modeling

Saturated soil has been modeled as a two-phase material base on Biot theory in which deformation for solid phase and fluid phase occur simultaneously. Soil mass during earthquake is affected by high intensity cycling loading. So, the soil mass should be modeled as a continuous environment with considering the interaction of solid and fluid phases [5].

In the present study, a saturated soil system based on a Biot theory two-phase system has been modeled for porous media. The numerical formulation of this method is known as u-p formulation, based on the assumptions including the constant of solid phase relative density in space and time, the constant porosity at time, the

incompressible particles of soil and the same acceleration in two solid and liquid phases [5].

In the u-p formulation, soil consists of three phases; liquid, solid and gas. For a fully coupled analysis, equilibrium or momentum balance for the soil-fluid mixture, momentum balance for the fluid phase, and mass balance for the whole system of soil and fluid must be satisfied. The uncertainties in this equilibrium problem are fluid displacement (u_s), displacement of the liquid phase relative to the solid phase (u_{rf}) and the liquid phase pressure (P). Note that the variables that have little or no effect on the problem were eliminated. Relatively, by eliminating the displacement of the liquid phase relative to the solid phase (u_{rf}), the number of equations of equilibrium problem is reduced to two. Since, the solid phase displacement equation and then the liquid phase displacement equation are located respectively, so these equations are called $u_s - P$ formulation, or $u - P$ formulation. The $u - P$ formula is presented in Eq. (1) [23]:

$$\begin{cases} M\ddot{U} + \int_v B^T \sigma' dV - QP - f^{(s)} = 0 \\ Q^T \dot{U} + HP + S\dot{P} - f^{(s)} = 0 \end{cases} \quad (1)$$

In the Eq. (1), M is the mass matrix, U is the solid displacement vector, B is the strain–displacement matrix, σ' is the effective stress matrix, Q is the gradient operator and flow equations, P is the pore water pressure vector, S is the matrix of compressibility and H is the permeability matrix. The vectors f^s and f^p include the effects of body forces, external loads and fluid fluxes, respectively. The soil was examined using the Yang multi-surface model with the help of the OpenSEES® Finite Element Software. Soil modeling is based on Yang method for the liquefiable soils. In this method, the simulation was based on the shear strain mechanism due to the liquefiable characteristics of sandy soil. The cone yielding surface of granular soils in the original stress space is shown in Fig. 1 [6].

For granular soils like sands, shear loading is directly related to the soil volume changes (dilatation and contraction). The boundary between expansion and contraction with the phase transformation (PT) surface, which is shown in Fig. 2.

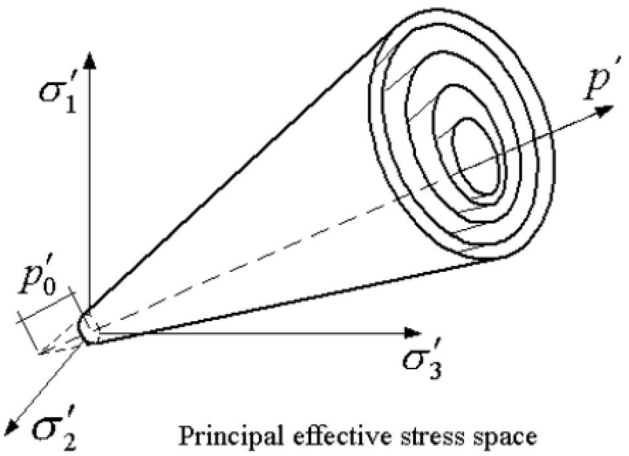

Fig. 1 Three-dimensional graph of the main effective stresses [6]

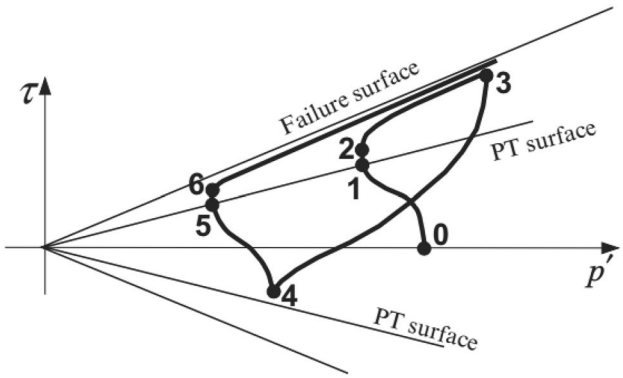

Fig. 2 Effective stress–strain diagram for shear stresses for granular soils [6]

2.2 Materials

The pressure-dependent, multi yield surface (PDMY) constitutive model implemented in OpenSEES has been used to simulate the nonlinear response of saturated sand. The OpenSEES user's manual suggest soil parameter values to use with loose sand (relative density of 15–35%, medium sand (35–65%), medium-dense sand (65–85%) and dense sand (85–100%) [3]. But there are no existing corrections between soil parameters and the relative density. So a relationship was derived based on the OpenSEES manual recommendations. The following formulas have been used based on the soil relative density [3] (Table 1):

where ρ is the mass density, p_r is the reference pressure, G_{max} is reference shear modules, B_{max} is reference bulk modules, φ is the friction angle, φ_{PT} is the phase transformation, N is the pressure dependent coefficient, c is contraction parameter, d_1 and d_2 are dilation parameters, l1, l2 and l3 are the liquefaction parameters, k_h and k_v are the horizontal and vertical coefficients of permeability, e is the porosity of the soil and θ is the Poisson coefficient of soil [3].

3 Modeling, loading, and boundary conditions

According to Fig. 3, the model consisted of a shallow foundation with 2-m width with 200 KN/m of linear load and it rested on 30 m of a liquefiable saturated sand soil which

Table 1 Relationships for PDMY parameters

Variable	Formula	Dr = 40%
$\rho\left(\frac{\text{ton}}{\text{m}^3}\right)$	$2.11(D_r)^{0.1567}$	1.828
G_{max}(kPa)	$G_r = 10500\frac{(2.17-e)^2}{1+e}P_r^{0.4}$	77,021.335
B_{max}(kPa)	$B_r = G_r\frac{2(1+\vartheta)}{3(1-2\vartheta)}$	359,432.922
φ(degree)	$\varphi = 16.2D_r + 25$	31.48
φ_{PT}(degree)	$\varphi_{PT} = 16.2D_r + 25$	31.48
p_r(kPa)	Constant	80
γ_{max}	Constant	0.1
N	Constant	0.5
c	$c = 0.0288D_r^{-1.4172}$	0.105
d1	$d_1 = 1.147D_r - 0.2454 \geq 0$	0.213
d2	$d_2 = 6.9686D_r - 1.7187 \geq 0$	1.069
l1	$l_1 = 10(D_r < 65\%)$ $l_1 = -35.484D_r + 32.5(D_r \geq 65\%)$	10
l2	$l_2 = -0.0154LnD_r - 0.0012$	0.013
l3	$l_3 = 1(D_r \leq 85\%)$ $l_3 = 0(D_r > 85\%)$	1
$k_h = k_v\left(\frac{m}{s} * 10^{-5}\right)$	–	5.9757
e	–	0.7
ϑ	–	0.4

is placed in a flexible container. This model was shaken with an earthquake (Fig. 4) with a peak ground acceleration of 0.16 g. The lateral boundaries perpendicular to the direction of shaking were constrained together to have the same displacement in the direction of shaking. The displacements of lateral boundaries parallel with the direction of shaking were tied in the direction perpendicular to the shaking. The bottom boundary was assumed fixed. Full dissipation of pore pressure was allowed through the surface of sand layer only and the lateral and bottom boundaries were considered to be impervious. The shallow foundation was modeled by rigid elements connected rigidly to the adjacent soil nodes. So in this study, the rough foundation assumption was adopted. The model has 2626 nodes and 2500 elements.

Considering that the effective time of the earthquake is in the range of 5–95% of the intensity (D5-95%) [17]; therefore, the results until 3th second have been neglected.

4 Results and discussion

4.1 Excess pore water pressure and r_u

The time history of the excess pore pressure in the free field and under foundation at depth of 4 m for middle sand layer with relative density of 40% were plotted in Figs. 5 and 6. Respectively. In the free field, the excess

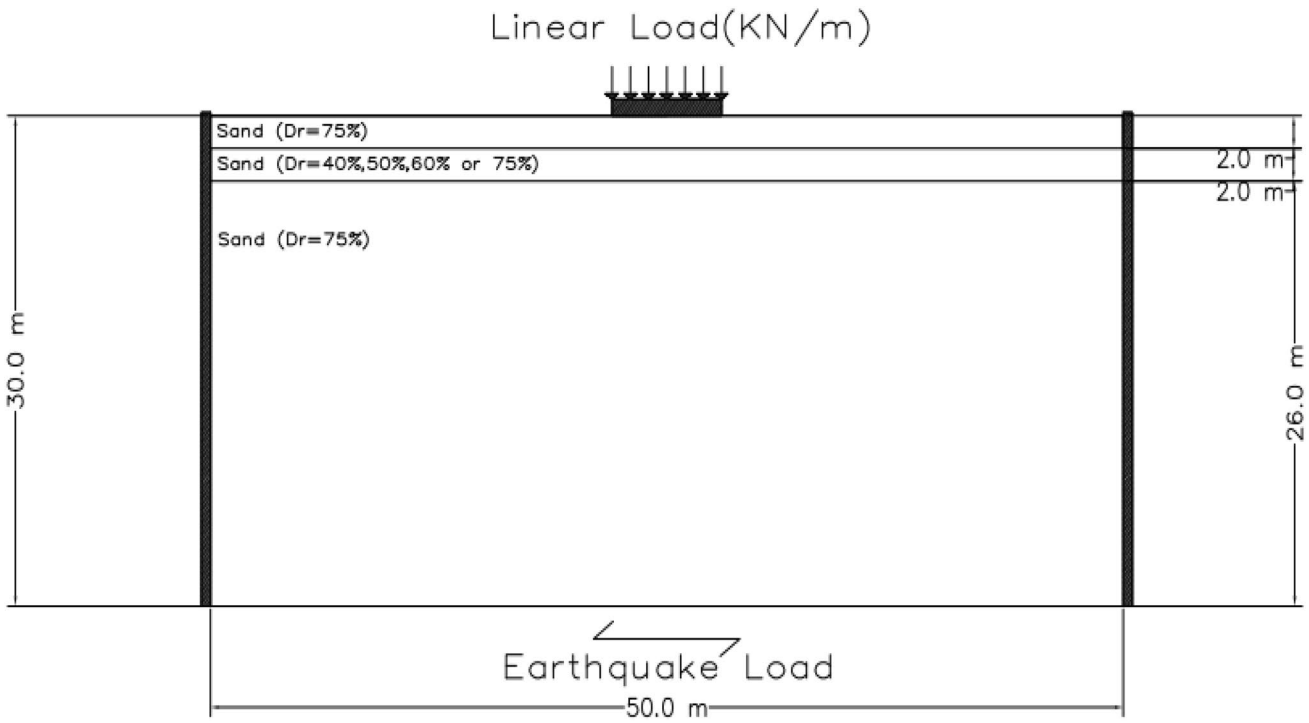

Fig. 3 Multi-layer soil box

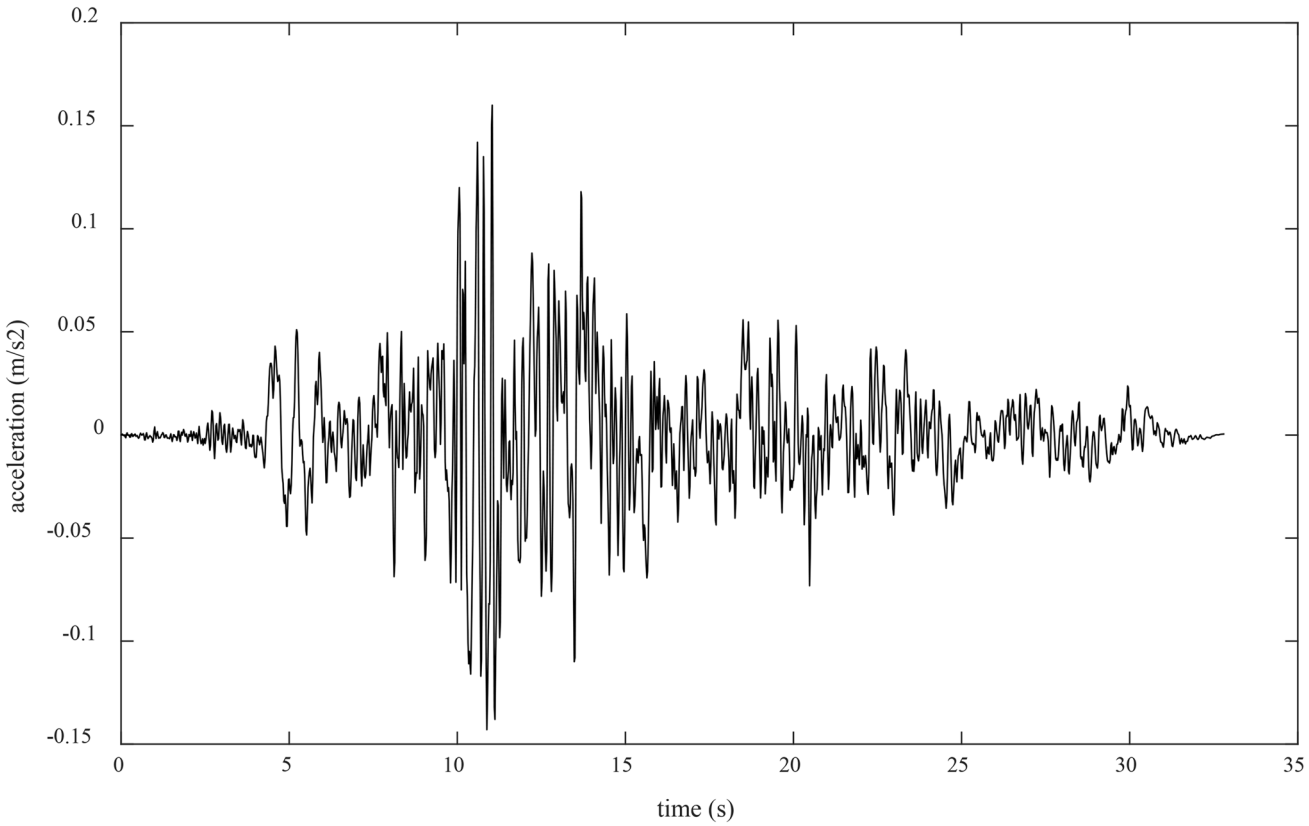

Fig. 4 Scaled time history of the input motion

pore pressure grows up until it reaches the peak value and then decreases gradually until the end of the shaking and after that the dissipation process occurs. It was observed that with increasing depth, the excess pore water pressure is going to increase. The excess pore water pressure increased until it reaches the time of the peak acceleration of the earthquake time history, and this state continues for 5 s and then gradually decreases. In the case of changes in the excess pore water pressure under foundation, it was observed that the excess pore water pressure increases along with the soil depth and reaches to the maximum point, and then gradually decreases. As it is seen in Fig. 6 at the depth of 4 m from the surface, the excess pore water pressure is negative, indicating the dilatation of the soil, but the state of the negative excess pore water pressure is not constant, and after 15th second, the excess pore water pressure becomes positive again. It is important to mention that along with the soil depth, the pore water pressure decreased. In addition, it should be noted that the value of excess pore water pressure for the different depth did not occur at the same time.

As shown in Fig. 7 on the free field, moments after 10th second, the value of r_u reaches approximately to $r_u = 1$ (which indicates the occurrence of liquefaction), and this situation continued until 18th second, and then gradually decreased which indicates the dissipation of the excess pore water pressure. It should be noted that under the foundation, the liquefaction did not occur because of the overburden loading.

Figure 8 shows the effect of the relative density of the middle sandy soil layer of the box and it shows that liquefaction has been occurred in shallow depth and non-liquefied state in deeper depths. It was observed that due to the soil layered system and the presence of a soil layer with low relative density, the excess pore water pressure in the depth of 2–5 m is increased, but then it has begun to decrease with increasing depth. This indicates that in lower densities, the pore water pressure of the underlying soil layer of the middle layer is released faster because of higher permeability. Note that this process is reduced by increasing the relative density of middle soil layer.

In the case of free field, according to Fig. 8 it is clear that to the depth of 6 m from the surface for all densities the excess pore water pressure ratio is between 0.95 and 1.0. Generally, with increasing the depth, the effect of overburden pressure from foundation reduced. The occurrence of liquefaction to the depth of 6 m indicates that even soils with an acceptable and high relative density

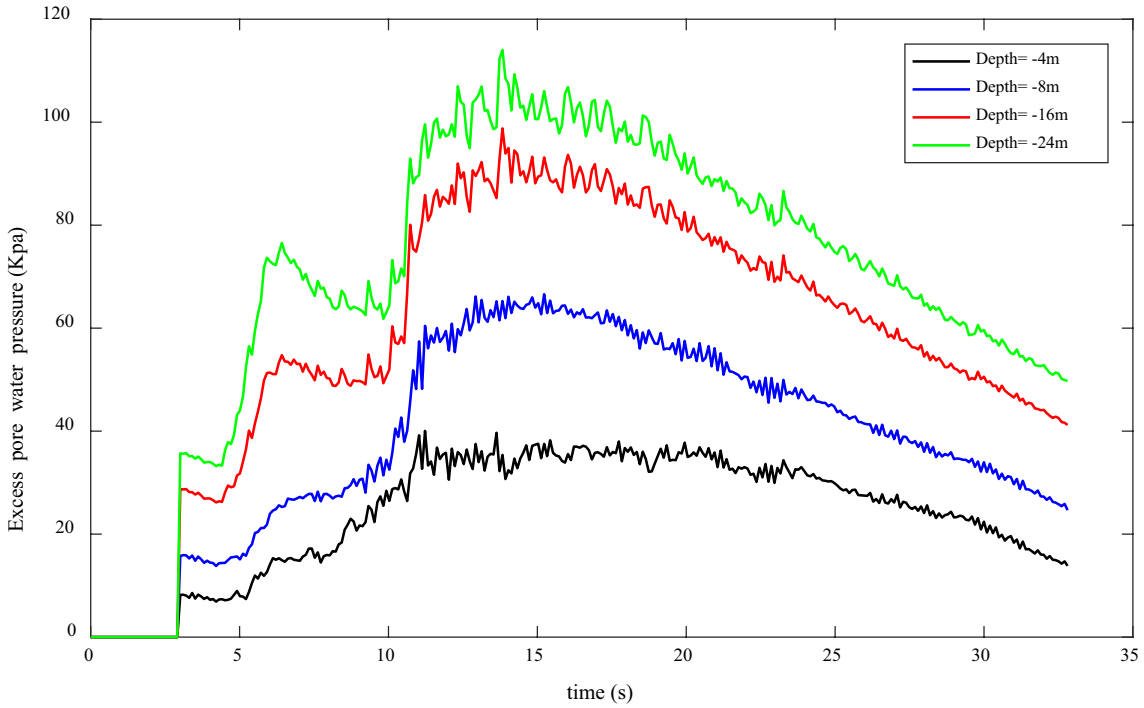

Fig. 5 Time history excess pore water pressure at different depths in free field

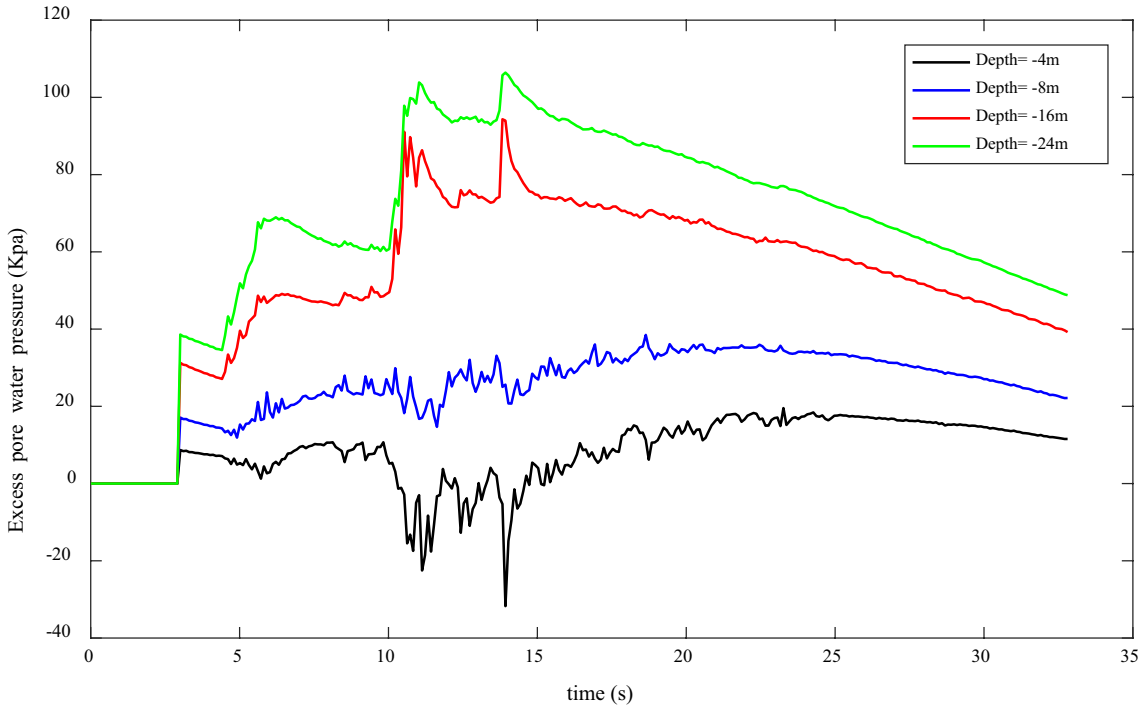

Fig. 6 Time history of excess pore water pressure at the different depths under the foundation

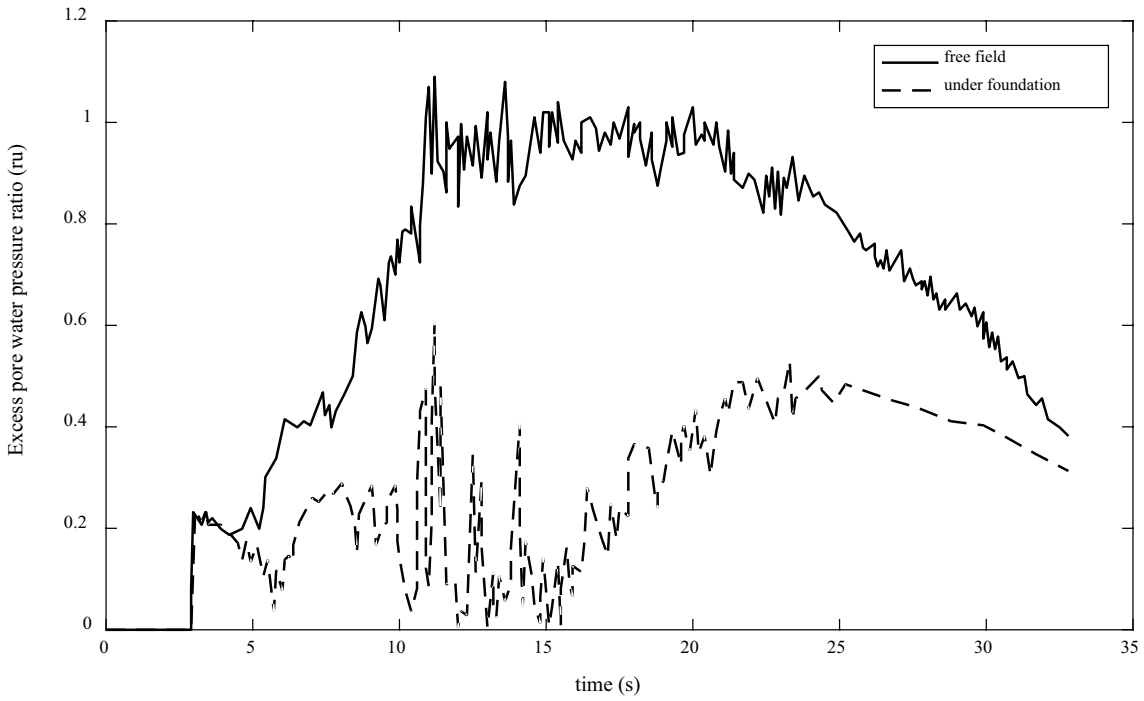

Fig. 7 Time history for r_u 4 m below the foundation and free field

are vulnerable to the occurrence of liquefaction phenomenon, and could be affected by the relative density of the adjacent layers, the intensity of the earthquake and other factors.

In Fig. 9, the time history of the excess pore pressure ratio under the foundation and free field for different relative density in the middle layer is graphed. It was observed that the changes in r_u under the foundation increased by increasing the relative density. In Fig. 9 the effect of Dr under overburden pressure is more obvious and for lower amounts of Dr according to the Fig. 9 the amount of r_u is lower, which indicates that with lower amount of permeability, water can dissipate faster under overburden pressure that has been imposed from shallow foundation. In other words, on the free field, the destructive effect of the underlying low-relative density layers does not appear well, as long as there is no overburden pressure form foundation or structures. Hence, conducting soil field experiments on the site before construction of the foundation (even for surface foundations) seems vital in order to prevent the destructive effect of the liquefaction phenomenon.

4.2 Settlement

By considering the occurrence liquefaction due to seismic load, the total settlement was around 21.32 cm at the end of the earthquake for Dr = 40% (in the middle layer). It should be noted that in this study, the settlement due to liquefaction was measured, which means that the static settlement due to the foundation loading has been lessened from total settlement.

Figure 10 shows the net settlement values due to the liquefaction for the different densities. By increasing the relative density of the middle soil layer, the amount of settlement has decreased. The maximum settlement occurred within a time interval of 10–15 s (more than 60% of the total settlement), and after 15th second, the actual settlement was not significant. In summary, Fig. 10 showed the effect of increasing relative density on the amount of settlement due to liquefaction.

By comparing the changes of settlement for different relative density (Fig. 11), it was observed when the relative density increased, the curve approached to the linear state and slope slowed down. However, the soil with a lower relative density (less than 60%) has a steep slope which lead to larger settlement. This indicates that a significant increase in settlement has been occured in the densities less than 60%.

5 Conclusion

In this study, the theory of Biot with using PDMY material in the OpenSEES software was employed, and the effects of relative density on the settlement of the saturated

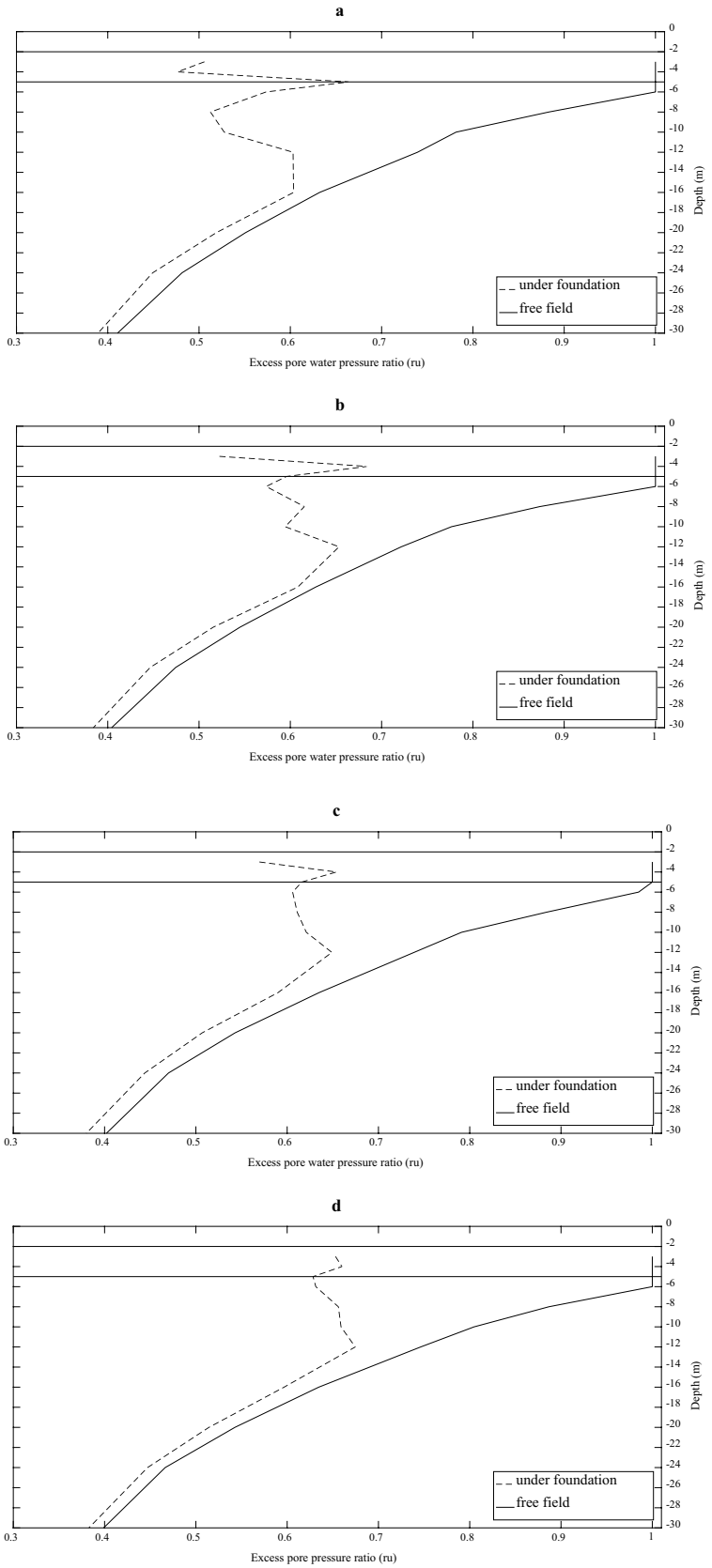

Fig. 8 Distribution of maximum excess pore pressure ratio along the soil depth at the foundation and free field for the soil layer with **a** Dr = 40%, **b** Dr = 50%, **c** Dr = 60%, **d** Dr = 75%

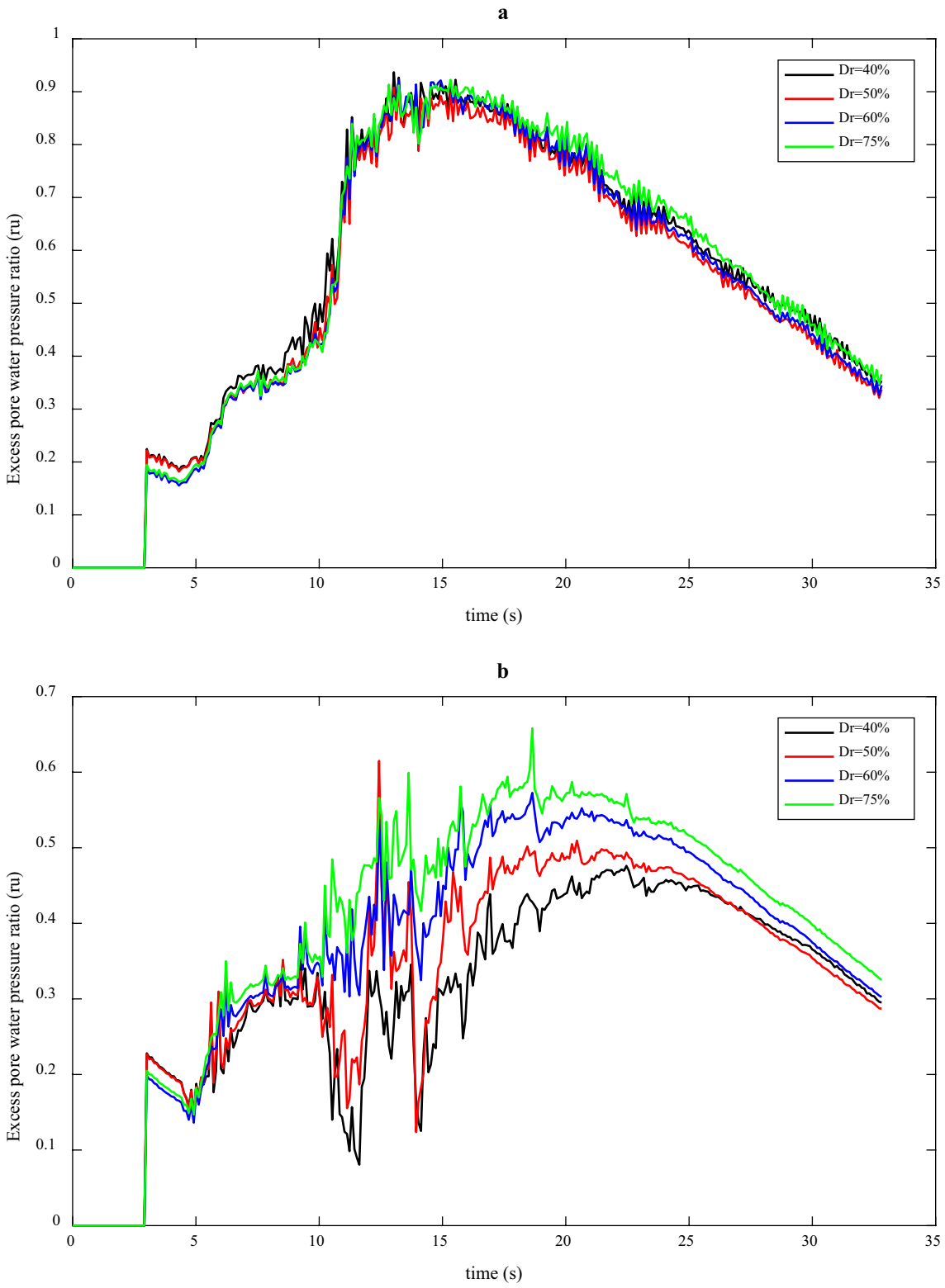

Fig. 9 Time history of excess pore water pressure ratios **a** free field, **b** under the foundation

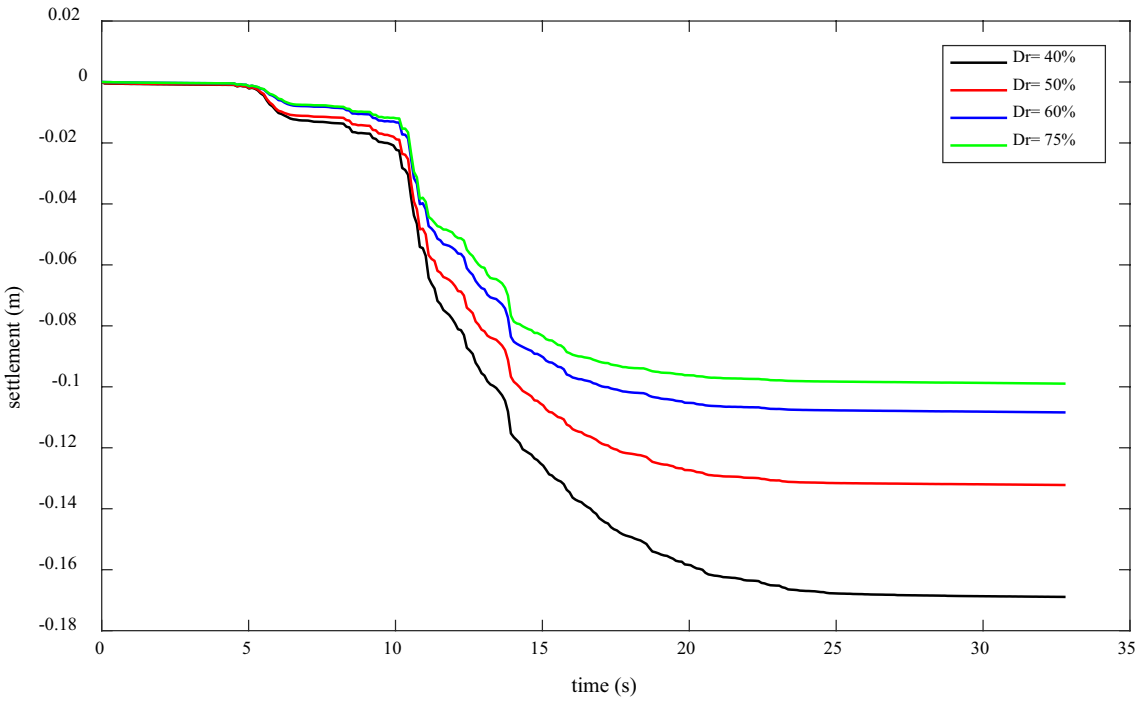

Fig. 10 Time history of settlement of foundation for different densities

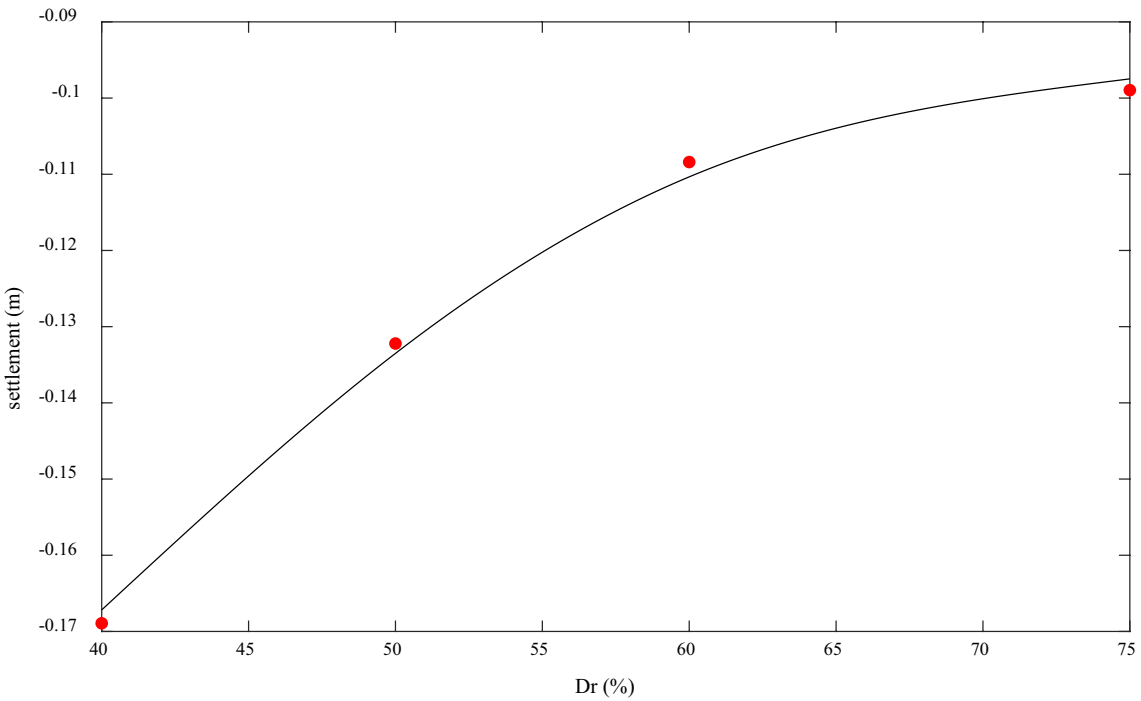

Fig. 11 The settlement–relative density curve for different relative densities

sandy soil due to the liquefaction was investigated. The excess pore water pressure, the ratio of the excess pore water pressure (r_u) and the settlement were also studied.

1. It was observed that the effect of the low-relative density soil layer on the sub-surface settlement is not significant. During earthquake, the low-relative den-

sity soil showed more liquefiable ability as it was predicted.
2. The probability of occurrence of liquefaction in saturated sandy soils around the low-relative density middle layer of the soil is expanded to the certain depth (which was found around 6 m) and below this depth the occurrence of liquefaction is highly unlikely (see Fig. 8).
3. More than 60% of the settlement occurred between 10th and 15th seconds of the earthquake time history, at this time interval the maximum acceleration values applied to the soil and eventually after 15th second, no significant settlement occurred.
4. Moreover, it was found that by increasing the relative density of liquefiable soil, the amount of settlement will decrease significantly.

Compliance with ethical standards

Conflict of interest The authors declare that they have no conflict of interest.

References

1. Ayoubi P, Pak A (2017) Liquefaction-induced settlement of shallow foundations on two-layered subsoil strata. Soil Dyn Earthq Eng 94:35–46. https://doi.org/10.1016/j.soildyn.2017.01.004
2. Biot MA (1962) Mechanics of deformation and acoustic propagation in porous media. J Appl Phys 33(4):1482–1498. https://doi.org/10.1063/1.1728759
3. Chen YW, Liu XQ, Dai HJ (2010) Free field analysis of liquefiable soils. Electron J Geotech Eng 15. www.ejge.com/2010/Ppr10.031.pdf
4. Dashti S, Bray JD, Pestana JM, Riemer M, Wilson D (2009) Mechanisms of seismically induced settlement of buildings with shallow foundations on liquefiable soil. J Geotech Geoenviron Eng 136(1):151–164. https://doi.org/10.1061/(ASCE)GT.1943-5606.0000179
5. Elgamal A, Lu J, Yang Z (2005) Liquefaction-induced settlement of shallow foundations and remediation: 3D numerical simulation. J Earthq Eng 9(spec01), 17–45.
6. Elgamal A (2007) Nonlinear modeling of large-scale ground-foundation-structure seismic response. ISET J Earthq Technol 44(2):325–339. home.iitk.ac.in/~vinaykg/Iset488.pdf
7. Fiegel GL, Kutter BL (1994) Liquefaction mechanism for layered soils. J Geotech Eng 120(4):737–755. https://doi.org/10.1061/(ASCE)0733-9410(1994)120:4(737)
8. Karimi Z, Dashti S (2015) Numerical and centrifuge modeling of seismic soil–foundation–structure interaction on liquefiable ground. J Geotech Geoenviron Eng 142(1):04015061. https://doi.org/10.1061/(ASCE)GT.1943-5606.0001346
9. Kawasumi H (1968) General report on the niigata earthquake of 1964. Tokyo Electrical Engineering College Press, Tokyo. https://trove.nla.gov.au/version/25158924
10. Kokusho T (1999) Water film in liquefied sand and its effect on lateral spread. J Geotech Geoenviron Eng 125(10):817–826. https://doi.org/10.1061/(ASCE)1090-0241(1999)125:10(817)
11. Koutsourelakis S, Prévost JH, Deodatis G (2002) Risk assessment of an interacting structure–soil system due to liquefaction. Earthq Eng Struct Dyn 31(4):851–879. https://doi.org/10.1002/eqe.125
12. Kumar A, Kumari S (2019) Numerical modeling of shallow foundation on liquefiable soil under sinusoidal loading. Geotech Geol Eng 37(2):517–532. https://doi.org/10.1007/s10706-018-0614-8
13. Liu H, Qiao T (1984) Liquefaction potential of saturated sand deposits underlying foundation of structure. In: Proceedings of the 8th world conference on earthquake engineering, San Francisco, CA, pp 21–28
14. Liu L (1992) Centrifuge earthquake modeling of liquefaction and its effect on shallow foundations. PhD Thesis, Department of Civil and Environmental Engineering; Rensselaer Polytechnic Institute, Troy, New York
15. Lopez-Caballero F, Farahmand-Razavi AM (2008) Numerical simulation of liquefaction effects on seismic SSI. Soil Dyn Earth Eng 28(2):85–98. https://doi.org/10.1016/j.soildyn.2007.05.006
16. Madabhushi GSP, Haigh SK (2010) Liquefaction induced settlement of structures. In: International conferences on recent advances in geotechnical earthquake engineering and soil dynamics, vol 5. http://scholarsmine.mst.edu/icrageesd/05icrageesd/session12/5
17. Makarios T (2015) Design characteristic value of the arias intensity magnitude for artificial accelerograms compatible with Hellenic seismic hazard zones. Int J Innov Res Adv Eng 2(1):87–98. www.academia.edu/download/36584233/14.JACE10085.pdf
18. Malvick EJ, Kutter BL, Boulanger RW (2008) Postshaking shear strain localization in a centrifuge model of a saturated sand slope. J Geotech Geoenviron Eng 134(2):164–174. https://doi.org/10.1061/(ASCE)1090-0241(2008)134:2(164)
19. Mehrzad B, Haddad A, Jafarian Y (2016) Centrifuge and numerical models to investigate liquefaction-induced response of shallow foundations with different contact pressures. Int J Civ Eng 14(2):117–131. https://doi.org/10.1007/s40999-016-0014-5
20. Maharjan M, Takahashi A (2013) Centrifuge model tests on liquefaction-induced settlement and pore water migration in non-homogeneous soil deposits. Soil Dyn Earthq Eng 55:161–169. https://doi.org/10.1016/j.soildyn.2013.09.002
21. Popescu R, Prevost JH, Deodatis G, Chakrabortty P (2006) Dynamics of nonlinear porous media with applications to soil liquefaction. Soil Dyn Earthq Eng 26(6–7):648–665. https://doi.org/10.1016/j.soildyn.2006.01.015
22. Reece F, Sanjana R, Nalini R, Jasim M (2017) Analysis of soil liquefaction using numerical modeling. In: International journal for research in applied science and engineering technology (IJRASET), vol 5, no X. www.ijraset.com. https://doi.org/10.22214/ijraset.2017.10011
23. Shahir H, Pak A (2010) Estimating liquefaction-induced settlement of shallow foundations by numerical approach. Comput Geotech 37(3):267–279. https://doi.org/10.1016/j.compgeo.2009.10.001